STUDY OF NEUTRON REACTIONS ON SOME ISOTOPES OF HYPERTHERMIA SAMPLES

AHMED HASSAN AZZAM [1], ISMAIL ABD-ELRAHEM ALI [1,2], GEHAN YOUSEF MOHAMED [1]

[1]Nuclear Physics Dept., Nuclear Research Center, Egyptian Atomic Energy Authority, Cairo, Egypt
[2] Nuclear Physics Dept. (Cyclotron Facility), NRC, EAEA, Cairo, Egypt
e-mail: gg_yousef@yahoo.com

Abstract

Thermal neutron capture cross-section of ^{26}Mg, ^{58}Fe, ^{64}Zn, ^{68}Zn, ^{152}Gd, ^{160}Gd were measured experimentally using the second Egyptian research reactor ETRR-2. Samples of ferrite $Mg(1-x)Zn_xFe_2O_4$ (where x=0.0, 0.2, 0.4, 0.6, 0.8 and 1) were previously synthesized by the sol–gel method, for use in some hyperthermia applications, and monitor (Zr) metallic foils were irradiated along with the samples by thermal neutrons. The induced activities in the samples were measured by high-resolution γ-ray spectrometry with a calibrated HPGe detector. The neutron capture cross-section of the reactions were determined relative to the reference cross section values for the ^{94}Zr(n,γ)^{95}Zr and ^{90}Zr(n,2n)^{89}Zr reactions as a single comparator. The present results were compared with the literature data, the TENDL-2021 database values and evaluated data, and in most of the cases a good agreement was found.

Keywords: *^{26}Mg, ^{58}Fe, ^{64}Zn, ^{68}Zn, ^{152}Gd, ^{160}Gd isotopes; Neutron capture cross-section; Off-line γ-ray spectrometry, Activation method*

Introduction

Mg–Zn ferrite is considered as one of the important materials with potential use in many applications [1-5]. Samples of ferrite $Mg(1-x)Zn_xFe_2O_4$ (where x = 0.0, 0.2, 0.4, 0.6, 0.8 and 1) were previously synthesized by the sol–gel method to be used in some hyperthermia applications [6, 7]. Introduction of minor concentration of the rare earth element Gd^{3+} may improve hyperthermia properties [8-12] and nuclear magnetic resonance image (NMRI) contrast [13].

In this work, the ferrite $Mg(1-x)Zn_xFe_2O_4$ samples with x = 0.2 were doped by Gd^{3+} with different compositions in order to be irradiated by neutrons using the second Egyptian research reactor ETTR-2. The irradiated samples were used for cross sections of (n,γ) reactions measuring and intercomparison for the ^{158}Gd, ^{160}Gd, ^{58}Fe, ^{64}Zn, ^{68}Zn, ^{26}Mg, as well as the (n,p) reactions of ^{54}Fe and ^{56}Fe isotopes. The (n,γ) reactions were produced through thermal neutron irradiation, while the (n,p) reactions of ^{54}Fe and ^{56}Fe were produced by using fast neutrons.

Natural gadolinium is used as a burnable poison in most Light Water Reactors, LWRs, to account for the excess of reactivity of fresh fuels. For an accurate prediction of the nuclear fuel cycle length, nuclear data and neutron capture cross sections must be known with a high precision [14].

The low abundance isotopes of some elements, in nature, are stable or have half-lives longer than several billion years. Since these isotopes have low abundance, poor nuclear data on their neutron capture cross sections are available. For some low abundance stable nuclei, there are no data available or, if exist there are large discrepancies between the few available data sets; especially, the cross sections of the thermal neutron capture reactions on ^{144}Sm, ^{152}Gd, ^{158}Dy, ^{168}Yb, and ^{184}Os are poorly measured. These data play a significant role in determining neutron capture cross sections over wide energy regions in nuclear data evaluations [15, 16].

To measure the capture cross section for ^{152}Gd and ^{160}Gd, the natural gadolinium foils (99.9% pure) were irradiated by using thermal neutrons from the ETRR-2 reactor and the gamma-ray activities were measured from the decay of ^{153}Gd and ^{161}Gd after neutron. In the natural gadolinium foil, ^{158}Gd is more abundant, and the capture cross section for this isotope was measured well with rather small uncertainties.

Experimental work

Samples preparation and irradiation

The samples of ferrite $Mg_{0.8}Zn_{0.2}Gd_yFe_{2-y}O_4$, where x = 0.0, 0.1, 0.2, 0.3, 0.4 and 0.6, y = 0.025, 0.05, 0.075 and 0.1, were synthesized by sol-gel method [3].

For irradiation of samples by the neutron flux in ETRR-2 research reactor, the samples and Zr monitor foils were placed in polyethylene vials and irradiated for short time (10 min), and long time (60 min), respectively.

The thermal and fast neutron fluxes were measured using Zr foils activation. After proper cooling times, the activities of the radioisotopes produced in the target and the monitor foils were measured, nondestructively, using high-purity germanium (HPGe) gamma-ray spectroscopy.

The acquisition data were collected by a multichannel analyzer (MCA) using Gamma vision (Version 5.1, EG&G ORTEC) software program. The HPGe detector used was a Canberra GC-6020 model with 60% efficiency and 2.9keV energy resolution at 1332.5 keV γ-ray line of ^{60}Co. The spectrometer was calibrated in energy and efficiency using standard point sources of ^{152,154,155}Eu, ^{137}Cs and ^{60}Co.

The nuclear data used for measuring the activity of ^{158}Gd, ^{160}Gd, ^{58}Fe, ^{65}Zn, ^{68}Zn and ^{26}Mg isotopes, respectively, are listed in Table 1.

The thermal neutron cross sections were calculated for ^{152}Gd(n,γ)^{153}Gd, ^{160}Gd(n,γ)^{161}Gd, ^{58}Fe(n,γ)^{59}Fe, ^{64}Zn(n,γ)^{65}Zn, ^{68}Zn(n,γ)^{69m}Zn and ^{26}Mg(n,γ)^{27}Mg reactions using thermal neutron flux calculated from ^{94}Zr(n,γ)^{95}Zr monitor, while for the neutron cross section calculation of ^{54}Fe(n,p)^{54}Mn and ^{56}Fe(n,p)^{56}Mn reactions, the fast neutron flux was determined by using the ^{90}Zr(n,2n)^{89}Zr monitor reaction.

Table 1. Nuclear data for the ^{158}Gd, ^{160}Gd, ^{58}Fe, ^{64}Zn, ^{68}Zn, ^{26}Mg, ^{90}Zr and ^{94}Zr isotopes, [14-16]

Irradiated isotope	Abundance (%)	Nuclear Reaction	$T_{1/2}$	γ-energies (keV)	Iγ (%)
^{26}Mg	11.03	^{26}Mg(n,γ)^{27}Mg	9.46 min	170.82	0.86
				843.76	71.80
				1014.52	28.20
^{153}Gd	0.2	^{152}Gd(n,γ)^{153}Gd	240.40 d	97.43	30.20
				103.18	22.10
^{160}Gd	21.86	^{160}Gd(n,γ)^{161}Gd	3.66 min	360.94	60.10
				314.92	22.70
				102.32	13.90
				283.55	5.91
^{58}Fe	0.28	^{58}Fe(n,γ)^{59}Fe	44.49 d	142.65	1.03
				1099.25	56.50
				1291.59	43.20
^{64}Zn	49.17	^{64}Zn(n,γ)^{65}Zn	243.93 d	1115.54	50.04
^{68}Zn	18.45	^{68}Zn(n,γ)^{69m}Zn	13.76 h	438.63	94.85
				573.01	0.033
^{54}Fe	5.85	^{54}Fe(n,p)^{54}Mn	312.20 d	834.85	99.98
^{56}Fe	91.75	^{56}Fe(n,p)^{56}Mn	2.58 h	846.76	98.85
				1810.73	26.90
				2113.09	14.20
Zr-foil (monitor)	^{94}Zr (17.38)	^{94}Zr(n,γ)^{95}Zr	64.03 d	724.19	44.27
				756.73	54.38
	^{90}Zr (51.45)	^{90}Zr(n,2n)^{89}Zr	78.41 h	909.10	99.04

Cross-section calculations

The reaction cross sections were calculated using the well-known activation formula. As input parameters, measured activity, flux, and number of target atoms per cm^2 are used. The experimental neutron cross-section σ_x for the nuclear reaction was calculated relative to the ^{94}Zr(n,γ)^{95}Zr and ^{90}Zr(n,2n)^{89}Zr monitor reactions using the following equation, [17, 18]:

$$\sigma_x = \sigma_m \frac{N_{p(x)}\varepsilon_m I_m \lambda_x N_m}{N_{p(m)}\varepsilon_x I_x \lambda_m N_x} \frac{(1-e^{-\lambda_m t_i})e^{-\lambda_m t_d}(1-e^{-\lambda_m t_c})}{(1-e^{-\lambda_x t_i})e^{-\lambda_x t_d}(1-e^{-\lambda_x t_c})} \quad (1)$$

where $N_{p(x)}$, $N_{p(m)}$ are the net peak area under the γ-ray peak of interest, ε is the detector efficiency, I is the γ-ray intensity, $N_{x,m}$ is the number of target or monitor nuclei, $(1-e^{-\lambda t_i})$ is the saturation factor, λ is the decay constant, t_i is the irradiation time, t_d is the cooling time, t_c is the measuring time, $e^{-\lambda t_d}$ is the decay factor, and $(1-e^{-\lambda t_c})$ is a term used for correcting the decay during the counting period. The subscripts x and m refers to the target and monitor reactions, respectively.

For the reactions (n, p) only average cross section could be measured and compared to that measured from previous works, and TENDL-2021 calculations.

The uncertainties associated with the measured cross sections include: counting statistics (2%-9%), detector efficiency (3%), neutron flux fluctuations (2%), monitor cross sections (2%), decay data (2%), and dead time (1.5%). The square root of the total in quadrature of all individual contributions for each of the formula's factors was used to calculate the uncertainty on the mesured cross-section. The total precentage error value was about 10% of the measured value.

Experimental procedure

Different samples of $Mg_{0.8}Zn_{0.2}Fe_{2-y}Gd_yO_4$ were prepared by sol–gel method with several Gd concentration ratios (y = 0.025, 0.05, 0.075 and 0.1). The components weight was carefully measured using a sensitive balance covered by thin Al foils. The samples were irradiated for two different irradiation times, T_i = 10 sec (short time), and T_i = 60 min (long time).

After the irradiation and a corresponding cooling time, the γ-ray activity for each sample was measured using high resolution HPGe detector for a reasonable time. The measured γ-lines were identified and attributed to each corresponding isotopes as indicated in Table 1. The detector efficiency curve was carefully measured at different source detector distances using γ standard sources. The exact γ-ray intensity (I_γ) of each line was calculated using the related efficiency value.

The thermal neutron flux value was measured by using the Zr(n,γ) reaction. The fast neutron flux, up to 10 MeV in energy, was estimated using the results of ^{90}Zr(n,2n)^{89}Zr reaction.

Results and discussion

^{26}Mg(n,γ)^{27}Mg reaction

The thermal neutron capture cross section (σ_0) values were obtained from the experimental analysis, after irradiation, using the research reactor and the previously described γ-ray spectrometer. The measured cross section value for ^{26}Mg(n,γ)^{27}Mg was found to be σ_0 = 37.3± 3.73 mb.

The results obtained for the thermal neutron capture cross section (σ_0) are presented in Table 2, and the comparison with previously measured data from literature [17-20] and TENDL-2021 database values is shown in Fig. 1.

Table 2. Neutron cross section for the ^{27}Mg, ^{59}Fe, ^{65}Zn, ^{69m}Zn, ^{153}Gd, ^{161}Gd, ^{54}Mn and ^{56}Mn isotopes

Target	Nuclear reaction	Cross section
^{26}Mg	^{26}Mg(n,γ)^{27}Mg	37.3±3.73 mb
^{58}Fe	^{58}Fe(n,γ)^{59}Fe	1300.1±130.0 mb
^{64}Zn	^{64}Zn(n,γ)^{65}Zn	750.0±75.0 mb
^{68}Zn	^{68}Zn(n,γ)^{69m}Zn	74.6±0.74 mb
^{152}Gd	^{152}Gd(n,γ)^{153}Gd	752.13±75.21 b
^{160}Gd	^{160}Gd(n,γ)^{161}Gd	1450.3±0.14 mb
^{54}Fe	^{54}Fe(n,p)^{54}Mn	295.2±29.5 mb
^{56}Fe	^{56}Fe(n,p)^{56}Mn	34.9±3.5 mb

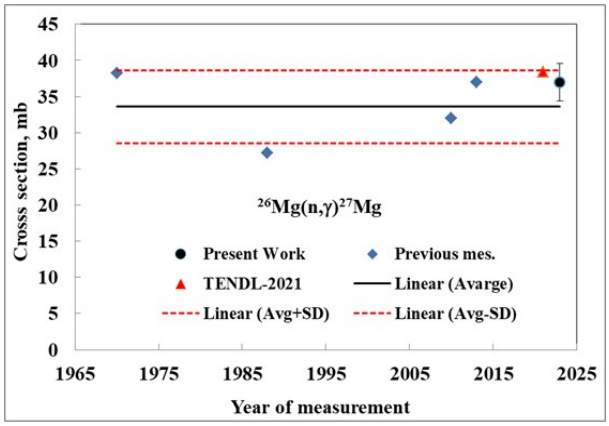


Fig. 1. Comparison of experimental values for thermal neutron capture cross-section of ^{26}Mg(n,γ)^{27}Mg reaction with previous measured and TENDL-2021 data

The dotted lines were used for the average value ± the standard deviation (SD) values of previous measured data. A good agreement was obtained for the thermal neutron cross-section experimental and evaluated values when comparing with averaged value of previous measured data (solid line), within the standard deviation.

^{58}Fe(n,γ)^{59}Fe reaction

The thermal neutron capture cross section (σ_0) value for the ^{58}Fe(n,γ)^{59}Fe reaction were found to be σ_0 = 1300.1 ± 130.0 mb. The thermal neutron capture cross section (σ_0) value is presented in Table 2, and the comparison with previously measured data from literature [17, 19-24] and TENDL-2021 database values is shown in Fig. 2.

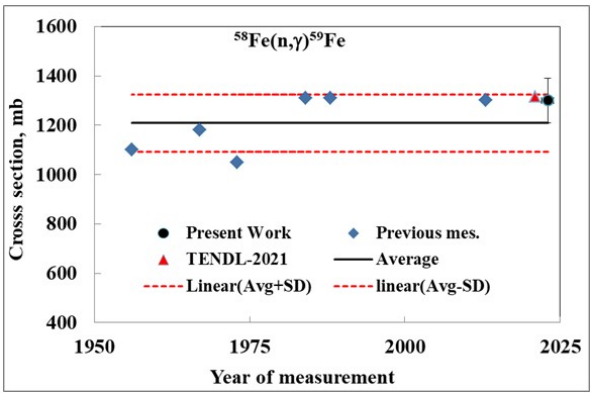


Fig. 2. Comparison of experimental values for thermal neutron capture cross-section of ^{58}Fe(n,γ)^{59}Fe reaction with previous measured and TENDL-2021 data

The experimental results are in good agreement with the averaged value of previous measured data and TENDL-2021 data values, within the standard deviation.

^{64}Zn(n,γ)^{65}Zn reaction

The thermal neutron capture cross section (σ_0) value is given in Table 2, and the comparison with previously measured data from literature [17, 19, 25-27] and TENDL-2021 database values is shown in Fig. 3.

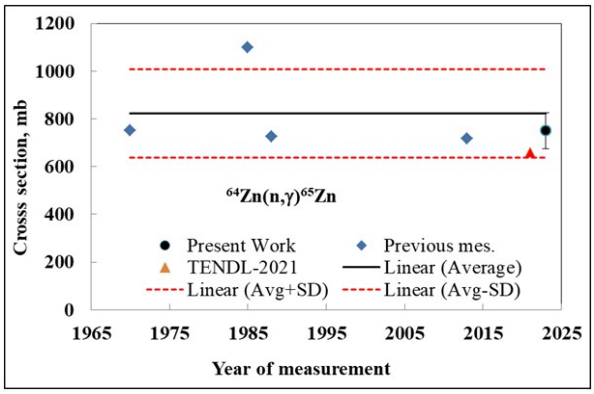


Fig. 3. Comparison of experimental values for thermal neutron capture cross-section of ^{64}Zn(n,γ)^{65}Zn reaction with previous measured and TENDL-2021 data

A good agreement was obtained for the thermal neutron cross-section experimental and evaluated values of the ^{64}Zn(n,γ)^{65}Zn reaction when comparing with the averaged value of the previous measured data (solid line), within the standard deviation as shown in the figure.

^{68}Zn(n,γ)^{69m}Zn reaction

The thermal neutron capture cross section (σ_0) values for the ^{68}Zn(n,γ)^{69m}Zn reaction were found to be σ_0 = 74.6 ± 0.74 mb. The thermal neutron capture cross section (σ_0) value is presented in Table 2, and the comparison with previously measured data from literature [17, 19-26, 49] and TENDL-2021 database values is shown in Fig. 4.

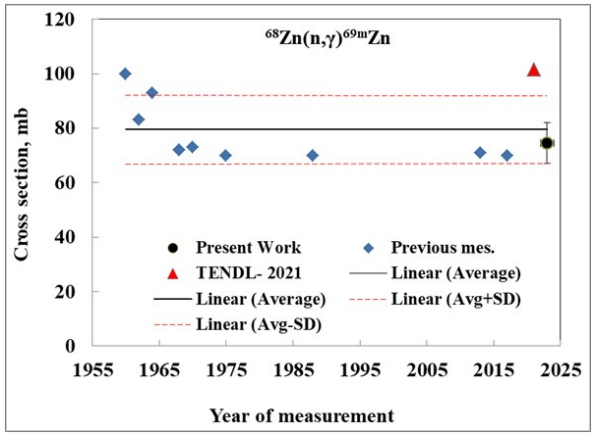


Fig. 4. Comparison of experimental values for thermal neutron capture cross-section of ^{68}Zn(n,γ)^{69m}Zn reaction with previous measured and TENDL-2021 data

The experimental results are in good agreement with the averaged value of previous measured data and TENDL-2021 data values, within the standard deviation.

^{152}Gd(n,γ)^{153}Gd reaction

The thermal neutron capture cross section (σ_0) value for the ^{152}Gd(n,γ)^{153}Gd reaction were found to be σ_0 = 752.12 ± 75.2 b. The thermal neutron capture cross section (σ_0) value is presented in Table 2, and the comparison with previously measured data from literature [13, 28, 29] and TENDL-2021 database values is shown in Fig. 5.

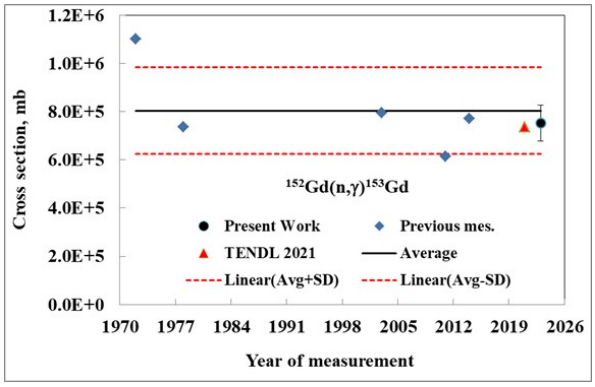


Fig. 5. Comparison of experimental values for thermal neutron capture cross-section of ^{152}Gd(n,γ)^{153}Gd reaction with previous measured and TENDL-2021 data

The experimental results are in good agreement with the averaged value of previous measured data and TENDL-2021 data values, within the standard deviation.

^{160}Gd(n,γ)^{161}Gd reaction

The thermal neutron capture cross section (σ_0) value for the ^{160}Gd(n,γ)^{161}Gd reaction were found to be σ_0 = 1450.3 ± 0.14 mb. The thermal neutron capture cross section (σ_0) value is presented in Table 2, and the comparison with previously measured data from literature [19, 30-33] and TENDL-2021 database values is shown in Fig. 6.

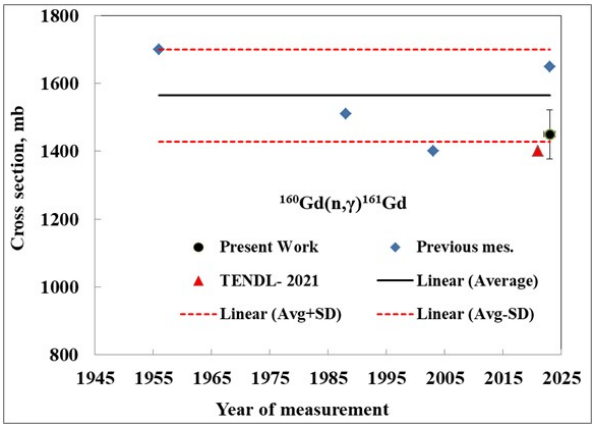


Fig. 6. Comparison of experimental values for thermal neutron capture cross-section of ^{160}Gd(n,γ)^{161}Gd reaction with previous measured and TENDL-2021 data

The experimental results are in good agreement with the averaged value of previous measured data and TENDL-2021 data values, within the standard deviation.

^{54}Fe(n,p)^{54}Mn reaction

Average cross section for fast neutron reactions were taken for neutron energies ranged from 1 to 10 MeV since fast neutron flux distribution ended at about 10 MeV [47, 48].

The average fast neutron cross section (σ) value was obtained from the experimental analysis using the irradiation in the fast neutron channel followed by direct gamma spectrum measurement. The fast neutron capture cross section (σ_0) values for the ^{54}Fe(n,p)^{54}Mn reaction were found to be σ_0 = 295.2±29.5 mb. The fast neutron capture cross section (σ_0) value is presented in Table 2, and the comparison with previously measured data from literature [34-44, 50] and TENDL-2021 database values is shown in Fig. 7.

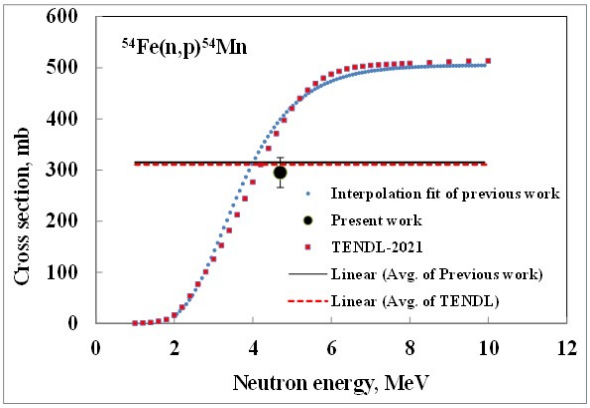


Fig. 7. Comparison of experimental values for fast neutron capture cross-section of ^{54}Fe(n,p)^{54}Mn reaction with previous measured and TENDL-2021 data

The experimental results are in good agreement with the averaged value of previous measured data and TENDL-2021 data values, within the experimental error.

^{56}Fe(n,p)^{56}Mn reaction

The fast neutron capture cross section (σ_0) values for the ^{54}Fe(n,p)^{54}Mn reaction were found to be σ_0 = 34.9±3.5 mb. The fast neutron capture cross section (σ_0) value is presented in Table 2, and the comparison with previously measured data from literature [34, 35, 38, 39, 44-48, 50] and TENDL-2021 database values is shown in Fig. 8.

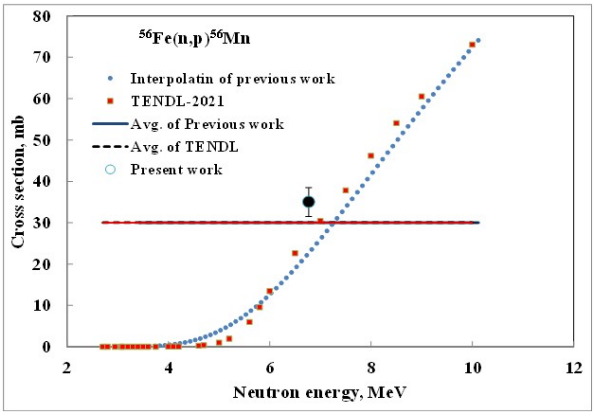


Fig. 8. Comparison of experimental values for fast neutron capture cross-section of ^{56}Fe(n,p)^{56}Mn reaction with previous measured and TENDL-2021 data

The experimental results are in good agreement with the averaged value of previous measured data and TENDL-2021 data values, within the experimental error.

Conclusions

Samples of ferrite $Mg(1-x)Zn_xFe_2O_4$ (where x = 0.0, 0.2, 0.4, 0.6, 0.8 and 1) were previously synthesized by the sol–gel method for use in some hyperthermia applications.

The activation method was used to measure the neutron capture cross-section of the nuclear reactions ^{26}Mg, ^{58}Fe, ^{64}Zn, ^{68}Zn, ^{152}Gd, ^{160}Gd (n,γ). After neutron irradiation, the induced activities in the samples and monitor (Zr) metallic foils were measured by high-resolution γ-ray spectrometer using a calibrated HPGe detector.

The neutron capture cross-section of the nuclear reactions of interest were determined relative to the reference cross section values for $^{94}Zr(n,\gamma)^{95}Zr$ and $^{90}Zr(n,2n)^{89}Zr$ neutron induced reactions.

The results were discussed and compared with a number of previous measured data and TENDL-2021 data base values. The experimental thermal neutron capture cross-section values obtained in present study were in good agreement with most of the previously measured data and TENDL data base values.

The average fast neutron cross section for the reactions $^{54}Fe(n,p)^{54}Mn$ and $^{56}Fe(n,p)^{56}Mn$ were measured and compared with the average calculated cross section values for neutron energies ranged from 1 to 10 MeV. The measured values were in good agreement with the calculated ones, within the experimental error.

References

[1] Jaison, D., Meher Abhinav, E., Gangwar, A., Kishore, P.N., Chandrasekaran, G., Mothilal, M. (2020) ″Effect of Gd3+ substitution on proton relaxation and magnetic hyperthermia efficiency of cobalt ferrite nanoparticles″, in *Mat. Res. Express*, vol. 7(6), ID 064009, https://doi.org/10.1088/2053-1591/ab9378.

[2] Hisham Alnasir, M., Awan, S., Manzoor, S. (2018) ″Magnetic and Magnetothermal Studies of Pure and Doped Gadolinium Silicide Nanoparticles for Self-Controlled Hyperthermia Applications″, *J. Magnetism and Magn. Materials*, vol. 449, pp. 137-144, https://doi.org/10.1016/j.jmmm.2017.10.026.

[3] Ji, B., Tian, C., Zhang, Q., Dongdong, J., Yang, J., Xie, J., Si, J. (2016) ″Magnetic properties of samarium and gadolinium co-doping Mn-Zn ferrites obtained by sol-gel auto-combustion method″, *J. Rare Earths*, vol. 34(10), pp. 1017-1023, https:// doi.org/10.1016/j.cjche.2020.08.024.

[4] Yadavalli, T., Raja, P., Ramaswamy, S., Chandrasekharan, G., Chennakesavulu, R. (2017) ″Proton Relaxivity and Magnetic Hyperthermia Evaluation of Gadolinium Doped Nickel Ferrite Nanoparticles as Potential Theranostic Agents″, *J. Nanosci. Nanotech.*, vol.16(2), pp.1–6, https://doi.org/10.1166/jnn.2017.12655

[5] Jadhav, S.V., Shewale, P.S., Shin, B.C., Patil, M.P., Kim, G.D., Rokade, A.A., Park, S.S., Bohara, R.A., Yu, Y.S. (2019) ″Study of structural and magnetic properties and heat induction of gadolinium-substituted manganese zinc ferrite nanoparticles for in vitro magnetic fluid hyperthermia″, *J. Colloid Interface Sci.*, vol. 541, pp.192-203, https://doi.org/ 10.1016/j.jcis.2019.01.063.

[6] El-Sayed, H.M., Ali, I.A., Azzam, A., Sattar, A.A. (2016) ″Influence of the magnetic dead layer thickness of Mg-Zn ferrites nanoparticle on their magnetic properties″, *J. Magnetism and Magn. Materials*, vol. 424, pp. 226-232, https://doi.org/ 10.1016/j.jmmm.2016.10.049.

[7] Ali, I.A., Mohamed, G.Y., Azzam, A., Sattar, A.A. (2017) ″Determination of concentrations of Fe, Mg, and Zn in some ferrite samples using neutron activation analysis and X-ray fluorescence techniques″, *Applied Rad. and Isotopes*, vol. 122, pp. 63-67, https://doi.org/10.1016/j.apradiso.2017.01.009.

[8] Thorat, N.D., Bohara, R.A., Tofail, S.A.M., Alothman, Z.A., Shiddiky, M.J.A., Hossain, S.A., Yamauchi, Y., Wu, K.C.W. (2016) ″Superparamagnetic Gadolinium Ferrite Nanoparticles with Controllable Curie Temperature – Cancer Theranostics for MR-Imaging-Guided Magneto-Chemotherapy″, *Europ. J. Inorg. Chem.*, vol. 2016(2), https://doi.org/10.1002/ejic.201600706.

[9] Raja, P., Yadavalli, T., Ravi, D., Therese, H.A., Ramasamy, C., Hayakawa, Y. (2017) ″Synthesis and magnetic properties of gadolinium substituted zinc ferrites″, *Mater. Lett.*, vol. 188, pp.406-408, https://doi.org/10.1016/j.matlet.2016.11.083.

[10] Leconte, P., Di-Salvo, J., Antony, M., Pepino, A., Hentati, A. (2012) ″Thermal neutron capture cross section of gadolinium by pile-oscillation measurements in MINERVE″, Conf. org. by American Nuclear Society, OSTI ID:22105767

[11] Kim, H.I., Herman, M., Mughabghab, S.F., Obložinský, P., Lee, Y.O. (2008) ″Evaluation of neutron cross sections for a complete set of Dy isotopes″, *Nuclear Instr. and Meth. in Phys. Res., Sect.B: Beam Interaction with Materials and Atoms*, vol. 266(16), pp. 3513-3528, https://doi.org/10.1016/j.nimb.2008.05.020.

[12] Lee, J.Y., Kim, Y., Kang, W., Kim, M.S., Sun, G.M. (2011) ″ Measurements of Thermal Neutron Capture Cross Sections of Low Abundance Stable Isotopes″, *J. Korean Phys. Soc.*, vol. 59(2), pp. 1932-1935, https://doi.org/10.3938/jkps.59.1932.

[13] Farina Arboccò, F., Vermaercke, P., Smits, K., Sneyers, L., Strijckmans, K. (2014) ″Experimental determination of k0, Q0 factors, effective resonance energies and neutron cross-sections for 37 isotopes of interest in NAA″, *J. Radioanal. Nucl. Chem.*, vol. 302, pp. 655–672, https://doi.org/10.1007/s10967-014-3281-0.

[14] Firestone, R.B., Ekstom, L.P. (2004) ″Table of radioactive isotopes″, Data base version 2.1., Lawrence Berkeley Nat. Lab., http://ie.lbl.gov/toi/index.asp.

[15] Brookhaven National Laboratory (1996) ″The NuDat program for nuclear data on the web″, vers. 2.4, in *Nudat*, Kinsey, R.R., Ed., http://www.nndc.bnl.gov/ nndc/nudat/.

[16] Brookhaven National Laboratory (2007) ″The NuDat program for nuclear data on the web″, vers. 2.5, in *Nudat2*, http://www.nndc.bnl.gov/nudat2/.

[17] Farina Arboccò, F., Vermaercke, P., Smits, K., Sneyers, L., Strijckmans, K. (2013) ″ Experimental determination of k0, Q0, Er factors and neutron cross-sections for 41 isotopes of interest in Neutron Activation Analysis″, *J. Radioanal. Nucl. Chem.*, vol. 296, pp. 931–938, https://doi.org/10.1007/s10967-012-2132-0.

[18] Nyarko, B.J.B., Sogbadji, R.B.M., Akaho, E.H.K., Agbemava, S.E. (2010) ″Cross section determination of short-to-medium lived nuclides in a low power research and an Am-Be neutron source″, IAEA Nucl. Data Section *report to the Intern. Nucl. Data Committee (INDC) No. 0574*, pp. 223-2320, ISSN 1454-2331.

[19] DeCorte, F., Simonits, A. (1988) ″A compilation of accurately measured 2200 m/s cross-sections for 101 n, gamma reactions of interest in activation analysis; a critical comparison with literature″, Proc. of Conf. on Nucl. Data for Sci. and Technol., p. 583, Mito, Japan.

[20] Ryves, T.B. (1970) ″Activation measurements of thermal neutron capture cross-sections and resonance integrals″, *Journal of Nuclear Energy*, vol. 24(1), pp. 35-42.

[21] Simonits, A., De Corte, F., Moens, L., Hoste, J. (1984) ″Critical evaluation and experimental determination of the nuclear activation and decay parameters for the reactions ^{50}Cr(n, ψ)^{51}Cr, ^{58}Fe(n, ψ)^{59}Fe, ^{109}Ag(n, ψ)^{110m}Ag″, *Journal of Radioanalytical and Nucl. Chemistry*, vol. 81, pp. 369–396, https://doi.org/10.1007/BF02135390.

[22] Alian, A., Born, H.J., Kim, J.I. (1973) ″Thermal and epithermal neutron activation analysis using the mono-standard method″, *J. Radioanal. Chem*., vol. 15, pp. 535–546, https:// doi.org/10.1007/BF02514270.

[23] Fabry, A., Deworm, J.P. (1967) ″Thermal Activation Cross-Section for the Reaction Fe-58(N,Gamma)Fe-59 in Natural Iron″, *Rep. from Euratom-countries + Euratom to EANDC No.76*, p.106.

[24] Takiue, M., Ishikawa, H. (1978) ″Thermal neutron reaction cross section measurements for fourteen nuclides with a liquid scintillation spectrometer″, *Nucl. Instrum. Meth.*, vol. 148(1), pp. 157-161.

[25] Koester, L., Knopf, K., Waschkowski, W., Kluever, A. (1985) ″Interaction of neutrons with zinc and its isotopes″, *Z Physik A*, vol. 320, pp. 661–668, https://doi.org/10.1007/BF01411868.

[26] Hogg, C.H., Wilson, W.L. (1970) ″Reactor thermal-neutron cross sections of 64-Zn,68-Zn, 121-Sb,123-Sb,55-Mn, and 186-W″, *Idaho Nuclear Corp. Reports No.1317*, p.53.

[27] Schuman, R.P., Tromp, R.L. (1970) ″Activation cross section measurements using the 2.0 keV, Sc filtered and 25 keV Fe filtered neutron beams″, *Idaho Nucl. Corp. Report No. 1317*, p.39.

[38] Steinnes, E. (1972) ″Resonance activation integrals of some nuclides of interest in neutron activation analysis″, *J. Inorg. Nucl. Chem.*, vol. 34(9), pp. 2699-2703.

[29] R.E. Heft, ″A consistent set of nuclear-parameter values for absolute instrumental neutron activation analysis″, Proc. of Conf. on Comp. in Activ. Analysis, p. 495, Puerto Rico.

[30] Kye, Yu., Shin, Sg., Cho, Mh., Namkung, W., Kim, G., Schillebeeckx, P., Paradela, C., Kopecky, S. (2020) ″Resonance parameters of Gd isotopes derived from capture measurements at GELINA″, *Eur. Phys. J. A*, vol. 56, art. 30, https://doi.org/ 10.1140/epja/s10050-020-00047-6.

[31] Leinweber, G., Barry, D.P., Trbovich, M.J., Burke, J.A., Drindak, N.J., Knox, H.D., Ballad, R.V., Block, R.C., Danon, Y., Severnyak, L.I (2006) ″Neutron Capture and Total Cross-Section Measurements and Resonance Parameters of Gadolinium″, *Nuclear Science and Engineering*, vol. 154(3), pp. 261-279, https://doi.org/10.13182/NSE05-64.

[32] Mangal, S.K., Gill, P.S. (1963) ″Thermal neutron activation cross-sections for isomer production (II)″, *Nuclear Physics*, vol. 41, pp. 372-379.

[33] Walker, W.H. (1956) ″The relative abundances and pile neutron capture cross sections of the isotopes of samarium, gadolinium, dysprosium and ytterbium″, PhD Thesis, McMaster University, Hamilton, Ontario.

[34] Filatenkov, A.A. (2016) ″Neutron activation cross sections measured at KRI in neutron energy region 13.4 - 14.9 MeV″, IAEA Nucl. Data Section, *USSR report to the Intern. Nucl. Data Committee (INDC) No.0460*.

[35] Viennot, M., Berrada, M., Paic, G., Joly, S. (1991) ″Cross section measurements of (n,p) and (n,np+pn+d) reactions for some titanium, chromium, iron, cobalt, nickel, and zinc isotopes around 14 MeV″, *Nuclear Sci. and Engin.*, vol.108(3), p.289, OSTI ID:5612504, https://doi.org/10.13182/NSE87-157.

[36] Lu, H.-L., Li, J.-Z., Fan, P.-G., Huang, J.-Z. (1989) ″Measurement of cross sections of reactions (n,p) and (n,a) for Fe-54 and Ta-181″. IAEA Nucl. Data Section, *Chinese report to the Intern. Nucl. Data Committee (INDC) No.16*.

[37] Meadows, J.W., Smith, D.L., Greenwood, L.R., Geraldo, L.P., Mannhart, W., Boerker, G., Mueller, G. (1991) ″Measurements of the neutron cross section for Fe-54(n,alpha)Cr-51 between 5.3 and 14.6 MeV″, Proc. of Conf. on Nucl. Data for Sci. and Technol., p.288, Juelich, Germany.

[38] Shimizu, T., Sakane, H., Shibata, M., Kawade, K., Nishitani, T. (2004) ″Measurements of activation cross sections of (n,p) and (n,alpha) reactions with d-D neutrons in the energy range 2.1 - 3.1 MeV″, *Annals of Nuclear Energy*, vol. 31(9), pp. 975-990.

[39] Mannhart, W., Schmidt, D. (2007) ″Measurement of neutron activation cross sections in the energy range from 8 MeV to 15 MeV″, *Phys. Techn. Bundesanst., Neutronenphys. Reports No.53*, OSTI ID:20948527.

[40] Paulsen, A., Widera, R. (1971) ″Ni-58(n,p)Co-58 and Fe-54(n,p)Mn-54 Cross-Section Measurements for Use as Threshold Detectors″, Proc. of Chemical Nucl. Data Conf., p.129, Canterbury, United Kingdom.

[41] Lauber, A., Malmskog, S.G. (1965) ″Measurements of the 54Fe(n,p)54Mn reaction cross section in the neutron energy range 2.3–3.8 MeV″, *Nucl. Phys.*, vol. 73(1), pp. 234-240.

[42] Salisbury, S.R., Chalmers, R.A. (1965) ″Fe54(n,p), (n,α), (n,2n) Cross Sections″, *Phys. Rev.*, vol. 140(2B), pp. 305–310.

[43] Carroll, E.E., Smith, G.G. (1965) ″Iron-54(n,p) Cross-Section Measurement″, *Nucl. Sci. Eng.*, vol. 22(4), pp. 411-415

[44] Smith, D.L., Meadows, J.W. (1975) ″Cross-Section Measurement of (n, p) Reactions for 27Al, 46,47,48Ti, 54,56Fe, 58Ni, 59Co, and 64Zn from Near Threshold to 10 MeV″, *Nucl. Sci. Eng.*, vol. 58(3), pp. 314–320.

[45] Liskien, H., Paulsen, A. (1965) ″Cross-section measurement for the threshold reactions 56Fe(n,p)56Mn, 59C(n,α)56Mn and 63Cu(n, 2n)62Cu between 12.6 and 19.6 MeV neutron energy″, *J. Nucl. Energy*, Parts A/B. Reactor Science and Technology, vol. 19(2), pp. 73–80.

[46] Terrell, J., Holm, D.M. (1958) ″Excitation Function for Fe56(n, p)Mn56″, *Physical Review*, vol. 109(6), pp. 2031–2035.
[47] Santry, D.C., Butler, J.P. (1964) ″Excitation Curves for the reactions Fe56(n, p)Mn56 and Co59(n, α)Mn56″, *Canadian Journal of Physics*, vol. 42(6), pp. 1030–1036.
[48] Ikeda, Y, Konno, C., Oishi, K., Nakamura, T., Miyade, H., Kawade, K., Yamamoto, H., Katoh, T. (1988) ″Activation cross section measurements for fusion reactor structural materials at neutron energy from 13.3 to 15.0 MeV using FNS facility″, *JAERI Reports No.1312*.
[49] Krane, K.S. (2017) ″Neutron capture cross sections of ^{70}Zn and the decay of ^{71m}Zn″, *App. Rad. and Isotopes*, vol. 121, pp. 28–37, https://doi.org/10.1016/j.apradiso.2016.12.029.
[50] Sublet, J.C., Fleming, M., Gilbert, M.R. (2017) ″From cutting-edge point wise cross-section to group wise reaction rate: A primer″, Intern. Conf. on Nuclear Data for Sci. and Technol., EPJ Web of Conferences, vol. 146, art. 02003, https://doi.org/10.1051/epjconf/201714602003.